Emission from Electronically Excited Metal Atoms during Single-Bubble Sonoluminescence

David J. Flannigan* and Kenneth S. Suslick†

Department of Chemistry, University of Illinois at Urbana-Champaign, Urbana, Illinois 61801, USA

(Received 21 April 2007; published 27 September 2007)

Variations in sonoluminescence (SL) from an acoustically driven but rapidly translating bubble in solutions of sulfuric acid with alkali-metal salts coincide with variations in translational bubble dynamics. At low acoustic pressures, emission from Ar excited states is observed and the bubble motion is smooth and elliptical. At elevated acoustic pressures, SL intensity *decreases*, emission from excited alkali-metal atoms is observed, and the bubble motion becomes increasingly erratic with frequent and abrupt changes in direction. These results provide a direct experimental link between single and multibubble SL and point toward the origins of sonochemical reactivity of nonvolatile species.

DOI: 10.1103/PhysRevLett.99.134301 PACS numbers: 78.60.Mq, 43.25.+y

Sonoluminescence (SL) and sonochemistry (SC) result from acoustic cavitation: the formation, growth, and implosive collapse of bubbles in a liquid irradiated with ultrasound [1]. Though SL and SC are by no means completely understood, the mechanisms leading to light emission and chemical reactions are now generally agreed upon; both originate from the intense compression of gas and vapor within the collapsing bubbles and the extreme temperatures and pressures that result. The light is due to emission from excited states of molecules and atoms and from radiative plasma processes [2,3], and chemical reactivity [4,5] arises from the high temperatures and pressure [6,7], which involve both the gas phase inside the bubble and the interfacial region between the bubble and the bulk liquid [8–10]. Quantitative descriptions of the molecular-level physical and chemical mechanisms of SL and SC, however, remain difficult due to the complex and dynamic nature of cavitation.

SL is commonly studied either from a single cavitating bubble (i.e., single-bubble sonoluminescence, SBSL) or from a cloud of cavitating bubbles (i.e., multibubble sonoluminescence, MBSL). Now that we better understand the conditions created during cavitation in each regime [6,7,11,12], interesting comparisons can be developed [13]. Quantification of the conditions generated during SBSL remained elusive until recently [11,12] largely due to the featurelessness of the emission spectra [14,15]. The observation of featureless spectra, narrow flash widths [16], and rapid bubble collapse [17] previously led to hypotheses of extraordinary conditions exceeding those generated within bubbles in a cavitation cloud [18,19]. Recent measurements of SBSL in sulfuric acid provide evidence for an optically opaque plasma core with emission temperatures $>15,000$ K [11]. In comparison, analyses of the spectral features observed during MBSL have shown that the effective temperatures and pressures generated are on the order of 5000 K and a few hundred bar [6,7,13]. Hydrodynamic models of cavitation suggest that the largest differences in intracavity conditions in SBSL vs MBSL may originate from diminished spherical symmetry during bubble implosion for the latter [20–22].

The hypothesis that SBSL can be considered as simply a hotter, more efficient version of MBSL has led to efforts to spectroscopically link the two phenomena [23–25]. We believe that unification of cavitation phenomena probably lies in the largely unexplored areas of moving SBSL (M-SBSL) and few-bubble SL [26,27]. M-SBSL is the first step from SBSL to MBSL by providing a single bubble with rapid translation, while still keeping it isolated from interactions with other bubbles or container walls. For this reason, we have examined the M-SBSL emission spectra from solutions of sulfuric acid (H_2SO_4) containing alkali-metal (e.g., Na, K) salts and noble gas coupled with stroboscopic studies of the corresponding bubble dynamics. While emission from excited alkali-metal atoms has been previously observed during MBSL [28,29], this is the first observation of such emission during SBSL, which provides a more ideal system for probing the mechanism leading to photon emission from nonvolatile species during SL. It is worth noting that Ohl has previously reported very weak Na atom emission from laser-initiated single-bubble collapse in aqueous NaCl solutions [30].

Emission from electronically excited alkali-metal atoms during SL presents an unresolved puzzle: how do the nonvolatile metal cations get heated in a collapsing bubble? There are two general proposals [23,29,31], but no prior experimental evidence to distinguish between them: a heated shell model or an injected droplet model, as illustrated in Fig. 1. In the heated shell model, the metal cations are reduced (perhaps by radicals produced in the gas phase of the collapsing bubble), heated, and excited in the interfacial region of the bubble. In the injected droplet model, microdroplets of liquid are nebulized into the interior of the bubble by capillary waves on or microjets from the bubble surface, thus providing a means for the nonvolatile components of the solution to enter the hot gas phase where the excited neutral alkali-metal atom would be created. The same two-site models have been used to explain the sono-

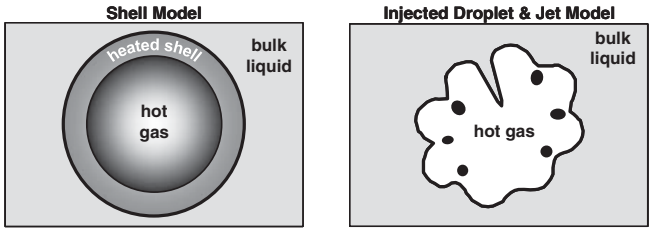

FIG. 1. Two possible two-site models of sonoluminescence and sonochemistry.

chemical reactions of nonvolatile precursors [5,8,32]. Hydrodynamic calculations by Kamath and co-workers suggest that a heated-liquid shell mechanism is unlikely to dominate [33].

Figure 2 shows M-SBSL spectra obtained at high acoustic driving pressure (apparent $P_a = 5.4$ bar [34,35]) from H_2SO_4 solutions of alkali-metal salts. The spectra show strong emission from excited alkali-metal atoms and an underlying continuum, the radiant power (Φ_{SL}) of which increases from the near-IR to mid-UV with a broad peak at ~270 nm. Weak satellite bands to the blue of the alkali-metal atom resonance lines (^2P) are also observed and are attributed to emission from an alkali-metal-Ar exciplex. This exciplex emission has been previously observed during rapid compression of alkali-metal vapor in a noble gas environment [36] and during MBSL from aqueous alkali-halide solutions [28,29]. The underlying continuum in Fig. 2 results from a combination of SO line emission ($B^3\Sigma^-$, $A^3\Pi$) and SO_2 quasicontinuum emission that is due to electronic transitions between several singlet and triplet excited states ($^1A_2$, $^1B_1$, $^3B_1$), all having excitation energies below 8 eV, and the ground state [37].

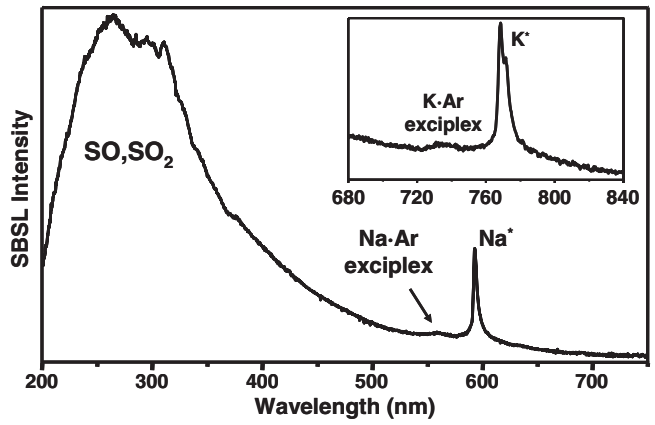

FIG. 2. M-SBSL from degassed 74% (by weight) H_2SO_4 containing 1.0% Na_2SO_4 and regassed with 50 torr Ar at $P_a = 5.4$ bar. The inset shows M-SBSL emission from degassed 74% H_2SO_4 containing 1.7% K_2SO_4 and regassed with 50 torr Ar. The spectra are labeled with the emitters responsible for the observed features. The spectrograph has been described elsewhere [26]. The spectra were corrected for the response of the optical system as well as absorption by the solution and the acoustic resonator.

The dependence of the M-SBSL spectra on P_a is remarkable. In Fig. 3, we show the M-SBSL emission spectra from an H_2SO_4 solution containing Na_2SO_4 and Ar gas over the range of P_a from 3.4 to 5.4 bar. At low P_a, a bubble can be formed and trapped, but does not emit. As the P_a is increased to ~3.4 bar, dim SL is observed, and the emission spectra consist of emission from Ar excited states (i.e., Ar*) with an underlying continuum attributed to radiative plasma processes [11,38]. As the P_a is increased further, Φ_{SL} increases more than 100-fold, while the spectral profile remains essentially unchanged save for broadening of the Ar lines. Further increases in P_a, however, result in dramatic changes in the spectral profiles and Φ_{SL}: at $P_a \sim 5$ bar, Φ_{SL} *decreases*, the emission from Ar* diminishes, and emission from neutral Na* is observed. Increasing the P_a to the maximum achievable (before the bubble is forced from the center of the resonator) increases the Na* emission line intensity and further decreases Φ_{SL}. With the onset of emission from Na*, the shape of the UV continuum emission also dramatically changes and corresponds to emission from electronically excited sonolysis products of H_2SO_4.

As demonstrated by the spectra in Fig. 4, a region of P_a exists between 4.4 and 5.2 bar where both Na* and Ar* emission can be observed. At first glance, this appears paradoxical, owing to the large disparity in the excitation energies of the populated states of these atoms: the energies of the emitting states of Ar are over 13 eV above the ground state (^1S_o), while the energies of the excited states of Na are only 2.1 eV above the ground state ($^2S_{1/2}$). Several mechanisms could account for the observation of Na* and Ar* emission in the same spectrum. For example, the two emitting species may be formed either at different times during or in different spatial locations within the

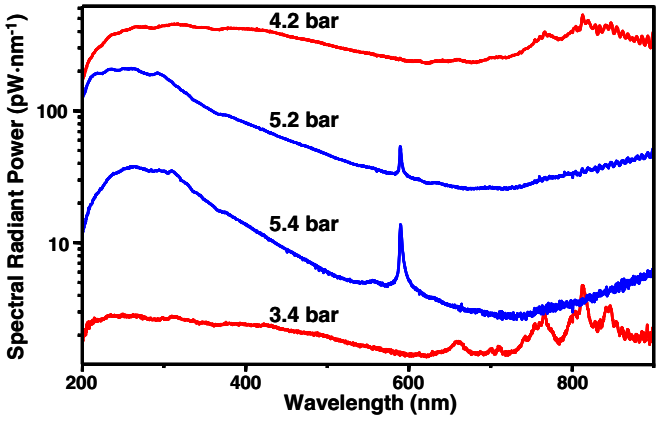

FIG. 3 (color online). M-SBSL from the same solution as in Fig. 1. All spectra were collected from the same bubble driven at different P_a, the magnitudes of which are labeled above the corresponding spectra. The features in the near-IR regions of the spectra generated at 3.4 and 4.2 bar (red online) arise from Ar* emission, while the feature at 590 nm in the spectra generated at 5.2 and 5.4 bar (blue online) arises from neutral Na* emission.

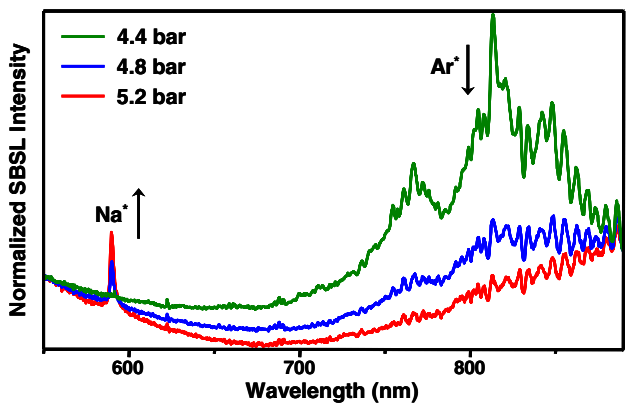

FIG. 4 (color online). M-SBSL spectra from 74% H_2SO_4 with 1.0% Na_2SO_4 and regassed with 50 torr Ar. The spectra have been normalized to SL intensity at 550 nm. The arrows next to the spectral features indicate how the intensities of the corresponding features change with increasing P_a relative to the underlying continuum.

collapsing bubble. Another possibility originates from the complex gas-phase chemistry that is occurring during bubble collapse where various types of collision-induced reactions (e.g., ionization, charge transfer, recombination, etc.) are likely to contribute to the observed spectra either directly or indirectly. Given the high temperatures and pressures generated during bubble collapse, rates of three-body processes cannot be neglected, which increases the range of reaction channels that must be considered.

In addition to spectroscopic characterization of M-SBSL, we have also quantified the macroscopic and microscopic bubble dynamics during M-SBSL via a stroboscopic technique [39]. As can be seen in Fig. 5, the changes in the spectral profiles and Φ_{SL} with increasing P_a coincide with changes in the bubble dynamics. As the P_a is increased, the translational velocity and the volume swept out by the moving bubble increase, while the expansion ratio (i.e., R_m/R_o, where R_m and R_o are the maximum and ambient bubble radii, respectively) decreases. These results are consistent with previous observations on similar systems [34,40]. The most significant observation, however, is a coupling of a substantial change in bubble dynamics with increasing P_a to the dramatic change in the M-SBSL spectra. As the SBSL spectra change from showing Ar^* emission to K^* emission lines, the macroscopic bubble motion changes from smooth and elliptical [Figs. 5(a) and 5(c)] orbits to increasingly erratic with frequent and abrupt changes in direction [Fig. 5(e)]. Because of the movement of the bubble in three dimensions, attempts to generate $R(t)$ curves of quality suitable for analysis with a Rayleigh–Plesset-type equation from the images obtained during strobing were unsuccessful. Thus, determination of an *effective* P_a and a collapse velocity was not possible with the techniques employed and may be the subject of future work.

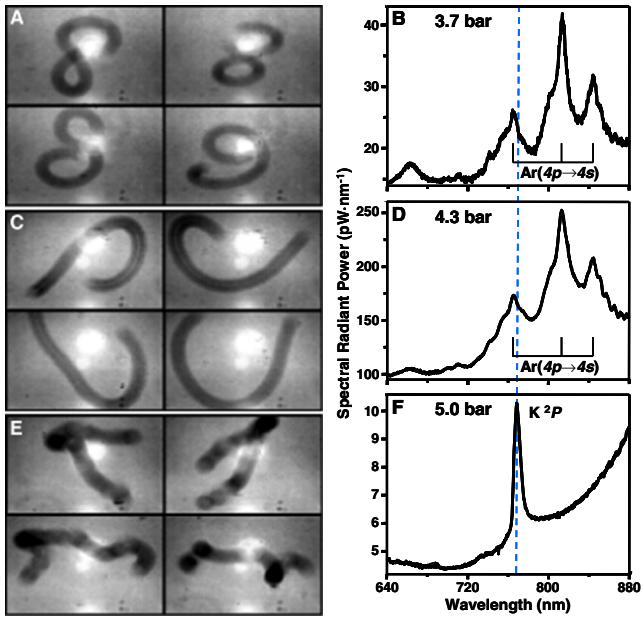

FIG. 5 (color online). Comparison of the bubble dynamics and corresponding M-SBSL spectra at different P_a: (a) and (b) at 3.7 bar, (c) and (d) at 4.3 bar, and (e) and (f) at 5.0 bar. The solution was 74% H_2SO_4 with 1.7% potassium pyrosulfate (Fisher Scientific) and 50 torr Ar. The imaging system and strobe technique have been previously described [26,39]; each frame is 1.28×0.80 mm with an exposure time of 66.67 ms; video of the bubble motion is available [42]. The translational bubble velocities were 34 and 38 mm $\cdot$ s^{-1} for (a) and (c), respectively, as determined by pixel counting. The erratic movement of (e) permitted only a rough estimate of 30 to 40 mm $\cdot$ s^{-1}. On average, the bubbles moved 1.1 and 1.3 μm per acoustic cycle for (a) and (c), respectively. The total volume swept out by bubble motion in (a) was estimated at 0.3 mm^3 and >2.2 mm^3 in (c) and (e). Maximum bubble radii (R_m) were estimated to be 50, 65, and 80 μm, while the ambient bubble radii (R_o) were estimated to be 10, 20, and 30 μm for (a), (c), and (e), respectively. Features in the spectra in (b) and (d) are due to Ar^* emission, while the feature in (f) is due to K^* emission. Spectra were collected immediately after image acquisition; the P_a at which the spectra were collected corresponds to the same P_a at which the images were acquired and is shown in the upper left corner of the spectra. The vertical line drawn through all three spectra (blue online) is aligned with the K^* emission line peak intensity at 770 nm. The increase in Φ_{SL} toward longer wavelengths is due to the low efficiency of the diffraction grating in this region ($\sim$ 20%).

The results shown in Fig. 5 indicate that the characteristics of M-SBSL emission are strongly dictated by the identity of the emitting species, which in turn are strongly correlated to the bubble dynamics. These observations support the hypothesis formulated by Matula *et al.* that attempted to explain differences between SBSL and MBSL spectra [23]: nonvolatile species are only able to enter the bubble when the macroscopic bubble motion becomes chaotic enough for energetic surface oscillations to de-

velop and thus entrain liquid droplets in the bubble interior [i.e., Fig. 1(b)]. Pyrolysis of the droplets then occurs during bubble implosion, which can lead to a variety of redox reactions capable of producing the excited state alkali-metal atoms. Droplet entrainment also explains why Ar^* emission and Φ_{SL} decrease with increasing P_a; the liquid droplets will lead to a lower peak temperature due to endothermic processes including liquid vaporization, excitation of bond rotations, and vibrations (i.e., reduction in the polytropic ratio), bond dissociation, and ionization [38,41].

We find that changes in M-SBSL spectra coincide with changes in the macroscopic bubble motion; at low P_a, we observe Ar^* emission lines and bubble motion that is smooth and elliptical, while at high P_a we observe emission from electronically excited alkali-metal atoms and bubble motion that becomes increasingly erratic with frequent and abrupt changes in direction. These results strongly suggest that droplet injection due to the development of capillary waves at the interface is the main mechanism for emission from excited nonvolatile species during SL.

By coupling studies of bubble dynamics with SL emission spectra from a single rapidly translating bubble in solutions of H_2SO_4 containing alkali-metal salts and Ar, we have uncovered a parameter space that allows for a direct link to be made between the traditionally studied SBSL and MBSL regimes. We have clearly shown that the main difference between these two distinct regimes lies in the macroscopic bubble motion, and that changes in the emission spectra coincide with changes in this motion. These results also have strong implications for the origins of sonochemical reactivity of nonvolatile species.

This research was supported by the NSF (No. CHE0315494).

*Current address: California Institute of Technology, Pasadena, CA, USA.
†ksuslick@uiuc.edu

[1] K. S. Suslick and L. A. Crum, in *Handbook of Acoustics*, edited by M. J. Crocker (Wiley, New York, 1998).
[2] M. P. Brenner, S. Hilgenfeldt, and D. Lohse, Rev. Mod. Phys. **74**, 425 (2002).
[3] S. J. Putterman and K. R. Weninger, Annu. Rev. Fluid Mech. **32**, 445 (2000).
[4] K. S. Suslick, Science **247**, 1439 (1990).
[5] K. S. Suslick *et al.*, Phil. Trans. R. Soc. A **357**, 335 (1999).
[6] W. B. McNamara III, Y. T. Didenko, and K. S. Suslick, Nature (London) **401**, 772 (1999).
[7] W. B. McNamara III, Y. T. Didenko, and K. S. Suslick, J. Phys. Chem. B **107**, 7303 (2003).
[8] M. Gutiérrez, A. Henglein, and C. H. Fischer, Int. J. Radiat. Biol. **50**, 313 (1986).
[9] K. S. Suslick, D. A. Hammerton, and R. E. Cline, Jr., J. Am. Chem. Soc. **108**, 5641 (1986).
[10] M. Ashokkumar *et al.*, J. Phys. Chem. B **101**, 10 845 (1997).
[11] D. J. Flannigan and K. S. Suslick, Nature (London) **434**, 52 (2005).
[12] D. J. Flannigan *et al.*, Phys. Rev. Lett. **96**, 204301 (2006).
[13] N. C. Eddingsaas and K. S. Suslick, J. Am. Chem. Soc. **129**, 3838 (2007).
[14] R. Hiller, S. J. Putterman, and B. P. Barber, Phys. Rev. Lett. **69**, 1182 (1992).
[15] R. A. Hiller, S. J. Putterman, and K. R. Weninger, Phys. Rev. Lett. **80**, 1090 (1998).
[16] B. Gompf *et al.*, Phys. Rev. Lett. **79**, 1405 (1997).
[17] K. R. Weninger, P. G. Evans, and S. J. Putterman, Phys. Rev. E **61**, R1 020 (2000).
[18] W. C. Moss, D. B. Clarke, and D. A. Young, Science **276**, 1398 (1997).
[19] K. Yasui, Phys. Rev. Lett. **83**, 4297 (1999).
[20] R. Löfstedt, B. P. Barber, and S. J. Putterman, Phys. Fluids A **5**, 2911 (1993).
[21] M. P. Brenner, D. Lohse, and T. F. Dupont, Phys. Rev. Lett. **75**, 954 (1995).
[22] L. A. Crum, J. Acoust. Soc. Am. **95**, 559 (1994).
[23] T. J. Matula *et al.*, Phys. Rev. Lett. **75**, 2602 (1995).
[24] D. Krefting, R. Mettin, and W. Lauterborn, Phys. Rev. Lett. **91**, 174301 (2003).
[25] J. B. Young, J. A. Nelson, and W. Kang, Phys. Rev. Lett. **86**, 2673 (2001).
[26] Y. T. Didenko, W. B. McNamara III, and K. S. Suslick, Nature (London) **407**, 877 (2000).
[27] C.-D. Ohl *et al.*, Phil. Trans. R. Soc. A **357**, 269 (1999).
[28] C. Sehgal *et al.*, J. Chem. Phys. **70**, 2242 (1979).
[29] E. B. Flint and K. S. Suslick, J. Phys. Chem. **95**, 1484 (1991).
[30] C.-D. Ohl, Phys. Fluids **14**, 2700 (2002).
[31] K. J. Taylor and P. D. Jarman, Aust. J. Phys. **23**, 319 (1970).
[32] A. Henglein, Advances in Sonochemistry **3**, 17 (1993).
[33] V. Kamath, A. Prosperetti, and F. N. Egolfopoulos, J. Acoust. Soc. Am. **94**, 248 (1993).
[34] S. D. Hopkins *et al.*, Phys. Rev. Lett. **95**, 254301 (2005).
[35] D. J. Flannigan and K. S. Suslick, Acoust. Res. Lett. Online **6**, 157 (2005).
[36] G. T. Lalos and G. L. Hammond, Astrophys. J. **135**, 616 (1962).
[37] J. M. Ajello *et al.*, J. Geophys. Res. **107**, 1099 (2002).
[38] D. J. Flannigan and K. S. Suslick, J. Phys. Chem. A **110**, 9315 (2006).
[39] Y. Tian, J. A. Ketterling, and R. E. Apfel, J. Acoust. Soc. Am. **100**, 3976 (1996).
[40] R. Toegel, S. Luther, and D. Lohse, Phys. Rev. Lett. **96**, 114301 (2006).
[41] W. B. McNamara III, Y. T. Didenko, and K. S. Suslick, J. Am. Chem. Soc. **122**, 8563 (2000).
[42] See EPAPS Document No. E-PRLTAO-99-051734 for videos of the bubble motion. For more information on EPAPS, see http://www.aip.org/pubservs/epaps.html.